

Low-energy insulating reconstructions of Si(111)-7×7 surface with and without stacking fault discovered by graph theory

Chaoyu He,^{1,2,*} Yuke Song^{1,2}, ShiFang Li^{1,2}, PeiZe Lin³, Jin Li^{1,2}, Tao Ouyang^{1,2} and Chao Tang^{1,2}

1. School of Physics and Optoelectronics, Xiangtan University, Hunan 411105, China;
2. Hunan Provincial Key Laboratory of Computational Condensed Matter Physics and Quantum Materials Engineering, Hunan 411105, China;
3. Institute of Artificial Intelligence, Hefei Comprehensive National Science Center, Hefei 230026, Anhui, China;

Electronic address: *hechaoyu@xtu.edu.cn;

The 7×7 reconstruction of Si(111) surface is one of the most fascinating configuration in nature, whose STM image has been well-understood by the famous dimer-atom-stacking-fault model (DAS). However, the electronic property of the DAS model is always confirmed to be metallic by first-principles calculations, while some experiments detected insulating features. It is still challenge to predict DAS-like reconstructions through traditional method to solve such a puzzle. Here, we show that 7×7 reconstructions can be quickly discovered by graph theory as implemented in the graph-space based RG² code for crystal structure prediction. Two groups of reconstructions with (DAS-d₈-T¹², DAS-d₈-T⁹H^{3-A}, DAS-d₈-T⁹H^{3-B} and DAS-d₈-T⁶H⁶) and without (AB-d₁₀-T¹², AB-d₁₀-T⁹H³, AA-d₁₀-T¹² and AA-d₁₀-T⁹H³) stacking-fault are discovered. They possess energetic stabilities comparable to the well-known DAS (DAS-d₈-T¹²) and show similar STM patterns, providing a plausible explanation for the experimentally observed 7×7 reconstruction on the Si(111) surface. The first-principles calculations show that DAS-d₈-T¹², DAS-d₈-T⁶H⁶, AB-d₁₀-T¹², and AA-d₁₀-T¹² are metallic, while DAS-d₈-T⁹H^{3-A}, DAS-d₈-T⁹H^{3-B}, AB-d₁₀-T⁹H³ and AA-d₁₀-T⁹H³ are insulating phases with gaps of 0.043 eV, 0.182 eV, 0.043 eV and 0.059 eV, respectively. Our work demonstrates the predictability of the Si(111)-7×7 reconstruction and provides the structural candidates for understanding the experimentally observed metal-to-insulator transition.

Crystal surface forms in the situation of periodicity-broken in one some given direction (hkl). Symmetry-broken and changes in coordination environment will enlarge the energy and make the surface energetically or dynamically unstable. Forced by low-energy principles, surface atoms will reconstruct with each other to lower the total energy and form different reconstructions. Such a phenomenon can happen in even the high symmetric (111) surface in covalent crystals, such as silicon, germanium, silicon carbide etc [1-5]. In the case of silicon, the 7×7 reconstruction of (111) surface has been attracted wide interests in the past decades [4-9] due to its fascinating STM pattern. Large number of experiments had been paid on investigations its atomic configurations and electronic properties [4-7]. As a large-size reconstruction, to

theoretically predict its atomic configurations is a big challenge [10-17] in condensed matter physics for any traditional crystal structure prediction methods. Some candidates for Si(111)-7×7 surface were guessed by imagination and constructed by hands [18-22]. The most famous one is the well-known dimer-adatom-stacking-fault model (DAS) proposed by K. Takayanagi and his co-workers in 1985 [23]. It was not until recent years that papers were published on methods capable of searching for the DAS structure [15-17]. The STM image of DAS model has been simulated by many groups, which can help us to understand the experimental results well. Thus, the atomistic model of DAS has been widely accepted as structural candidate for Si(111)-7×7 reconstruction in further theoretical investigations [24-36].

In views of electronic property, the metallic features of DAS are consistent with the experimental results obtained by photoemission and scanning tunneling spectroscopy (STS) at room temperature [37-39], as well as some low-temperature photoemission measurements [40-42]. However, they are in contrast with the insulating features [7, 43] detected in low-temperature photoemission spectra [37], as well as the hard or soft energy gaps observed below 20K in STS spectra [44-45], and inferred from charge transport experiments [46]. In order to continue using the metallic DAS mode, the soft energy gap is understood by long-range interaction induced V-shaped Coulomb gap [47] and the hard energy gap of about tens of meV is explained as the enhanced soft Coulomb gap due to local Coulomb blockade effects [44-46]. However, modified calculations such as DFT+U approximations and spin-split calculations also show that DAS is still a metallic phase [7]. Vertical displacements of adatoms had also been considered in previous calculations [7], but the calculated band structures can't explain the metal-insulator transition.

In principle, theoretical calculations are always incorrect if they do not agree with the experimental results. For first-principles calculations, the PBE-version functional usually underestimates the split-energy crystalline-field and under-determinates the band gaps of semiconductors. This may one of the possible reason the DAS model can't explain the insulating features reported in Si(111)-7×7 surface reconstruction. However, the high-level HSE06-based functionals [48] and GW approximations [49] are too expensive to solve this problem. Another possible reason is that the DAS model is not the only one structural candidate for reconstructed Si(111)-7×7 surface [50-52]. Maybe there are some low-energy insulating phases reconstructed directly from the clean surface or from the DAS model. Recently, J. E. Demuth proposed a digitated faulted adatom (DFA) model to replace DAS using for explaining Si(111)-7×7 surface reconstruction [51-52]. But such a new DFA model has been quickly commented by other researchers due to its instability [53]. Thus, we need some other new reconstructed models to fix the unsolved issues in Si(111)-7×7 surface. However, to theoretically solve the crystalline configuration of such a large-size reconstruction is still a big challenge for traditional method for crystal prediction. Special and advanced technologies [15-17, 54] are expected for dealing with this type of problems.

In this work, the graph theory as implemented in RG² code [54] is employed to search possible reconstructions of Si(111)-7×7 surface. Such a method in RG² has important advantages in handling large structure prediction [55] and has achieved numerous results in structural prediction [56-58]. Beyond the well-known DAS model of DAS-d₈-T¹², some new reconstructed configurations for Si(111)-7×7 surface has been successfully discovered by graph theory in RG² code, including the DAS like models (DAS-d₈-T¹², DAS-d₈-T⁹H^{3-A}, DAS-d₈-T⁹H^{3-B} and DAS-d₈-T⁶H⁶) and non-DAS models (AB-d₁₀-T¹², AB-d₁₀-T⁹H³, AA-d₁₀-T¹² and AA-d₁₀-T⁹H³), with and without stacking-fault, respectively. All these new models possess similar surface morphology to the famous DAS model (DAS-d₈-T¹²), but with different atomic configurations in details. Their calculated surface-energies are close to each other under the framework of PBE-based first-principles calculations, indicating similar stabilities. Furthermore, these models show also similar STM images to that of the well-known DAS-d₈-T¹², all match the reconstructed Si(111)-7×7 surface in atomic level views. The most interesting thing is that, according to our first-principles calculations, DAS-d₈-T¹², DAS-d₈-T⁶H⁶, AB-d₁₀-T¹², and AA-d₁₀-T¹² are metallic phases, while DAS-d₈-T⁹H^{3-A}, DAS-d₈-T⁹H^{3-B}, AB-d₁₀-T⁹H³ and AA-d₁₀-T⁹H³ are insulators with intrinsic band gaps of 0.043 eV, 0.182 eV, 0.043 eV and 0.059 eV, respectively. Our results demonstrate the predictability of the Si(111)-7×7 reconstruction by graph theory and provides two potential insulating candidates for understanding the metal-insulator transition in such a mysterious surface of Si(111)-7×7 surface.

It is necessary to discuss the principles of reconstruction before searching new possible candidates. Symmetry-broken and changes in coordination make the surface unstable in energy and it will reconstruct to lower the energy of the system. Two widely accepted roles, the chemical dangling bonds and the geometrical distortions, are the two important roles for determining the surface energy. Less dangling bonds and small distortions always mean low energy. The clean Si(111) surface possesses one dangling bond in its unit cell (uc) and it can't reconstruct to other configurations due to the constraints of periodicity and symmetry. In proper super-cells, such as the hexagonal $\sqrt{3}\times\sqrt{3}$ cell, one additional adatom on the tetragonal position (T4) will saturate all the three dangling bonds at the surface. Although it will introduce one additional dangling bond and three distorted atomic bonding environment, such a fully-covered $\sqrt{3}\times\sqrt{3}$ -supercell becomes more stable in energy. In large-cells, such as 5×5 and 7×7 which can't be fully-covered by adatoms, dimerizations in inner atoms are further considered cooperating with adatoms to forming the well-known DAS model with lower surface energy. However, the DAS models can only be promoted to the (2n+1)×(2n+1) super cells and the inter-layer stacking-fault in discontinuous small triangular area makes it difficult to be understood in dynamics and statistical mechanics views [64].

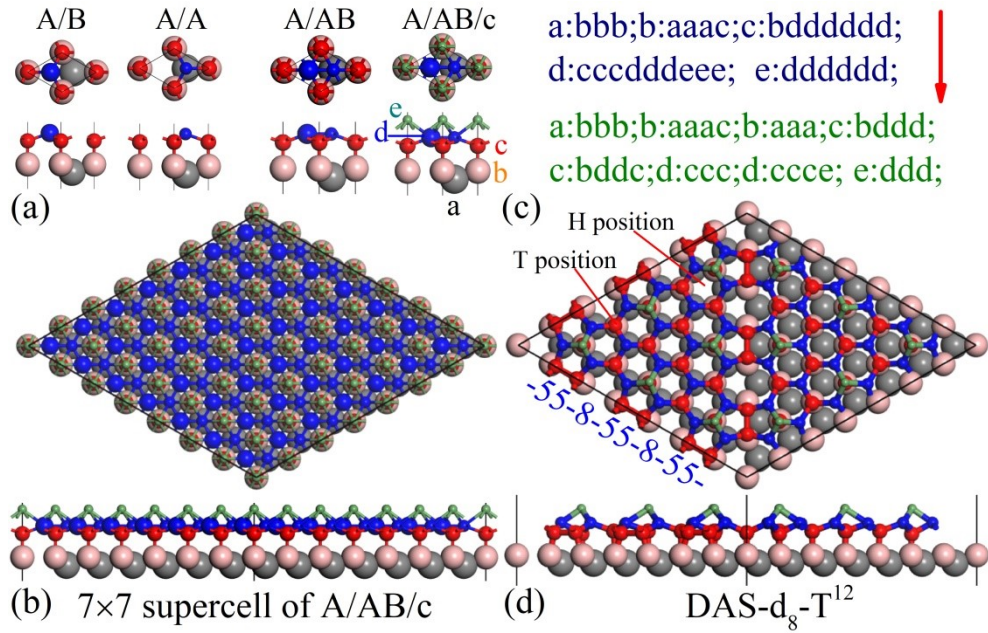


Fig.1. (a) The two fundamental stacking manners (A/A and A/B) in silicon bilayer and the hypothetical stacking manner without (A/AB) and with (A/AB/c) fully covered adatoms at the T4 (T) and hexagonal (H) positions. (b) the 7×7 supercell of A/AB/c model. (c) The adjacent relationships in the hypothetical A/AB/c (blue) and the reconstructed candidates (green). (d) The well-known DAS model for Si(111)- 7×7 surface (DAS-d₈-T¹²).

To find low energy reconstruction for Si(111)- 7×7 surface, a graph-based strategy is proposed and implemented by RG² code[54]. As shown in Fig. 1 (a) are the two fundamental stacking in silicon-bilayers, A/A and A/B. Here, we hypothetically constructed a hybridized one (A/AB) with fully covered adatoms in the T4 (T) and hexagonal (H) positions (A/AB/c), whose 7×7 supercell will be considered as starting point for reconstruction in RG². The five layers of atom in A/AB/c are labeled as a, b, c, d and e from inside to outside as shown in the picture, where the silicon layer formed by a and b are fixed for matching the bulk phase in the whole process. The adjacent relationships in this model can be easily featured as a:bbb, b:aaac, c:bbbbbb, d:ccccdeee and e:dddddd, where a:bbb means that atom a connected to 3 atoms labeled as b. The principles to construct low-energy reconstructions can be summarized as follows: Remove as many surface atoms d as possible to reduce the number of dangling bonds. Create possible self-saturation between the inner atoms c that lose surface atoms. Retain as many adsorbed atoms e as possible to saturate the surface atoms d. Remove a small number of inner atoms c, translating the dangling bonds to the next inner layer. RG² can accomplish these tasks quickly. It will load the 7×7 supercell of A/AB/c and calculate its hexagonal symmetry subgroup (Nos.143 and 156) at the first step. And then, it randomly removes a small number of atoms labeled as c, as well as a large number of atoms labeled as d and e, under the constraints of subgroup symmetry. Finally, RG² will build the quotient graph (QG) for the rested framework and optimized the configurations with accepted adjacent relationships as listed in Fig1 (c). Those unlisted adjacent relationships are higher energy ones and not considered in this work. Here, a:bbb

means atoms a with fixed positions for connecting bulk phase; b:aaac and b:aaa indicate the fixed atoms b for linking the surface layer, with and without new introduced dangling bonds, respectively; c:bddd and c:bddc are the adjacent relationships for atoms c in the surface layer with and without self-saturated dimerization, respectively; d:ccc and d:ccce indicate the rested atoms d in the outset surface layer with and without dangling bonds; And e:ddd means the rested adatoms e used for saturating the dangling bonds on the outset surface atoms d.

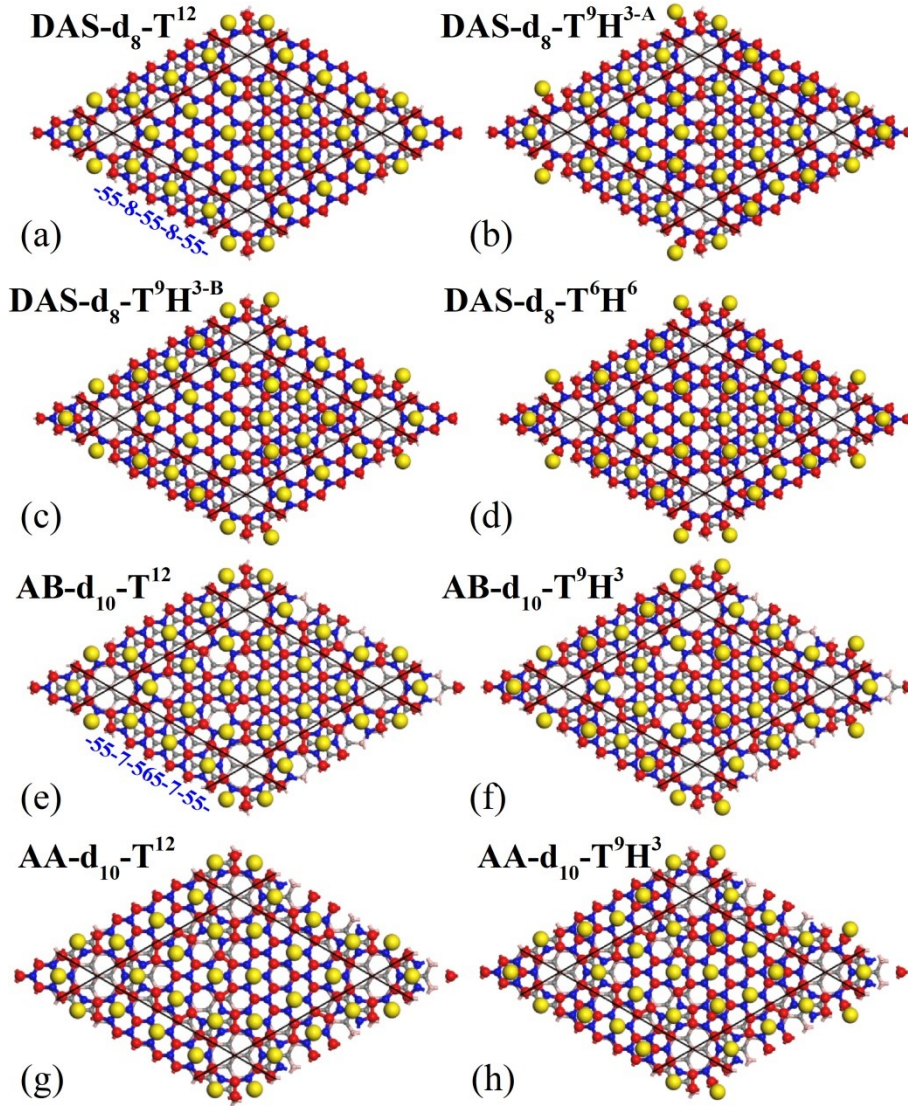


Fig.2. (a)-(d) are the DAS models DAS-d₈-T¹², DAS-d₈-T⁹H^{3-A}, DAS-d₈-T⁹H^{3-B} and DAS-d₈-T⁶H⁶. (e)-(h) are the non-DAS models AB-d₁₀-T¹², AB-d₁₀-T⁹H³, AA-d₁₀-T¹² and AA-d₁₀-T⁹H³. Adatoms are marked as big yellow balls.

This approach is highly effective. It can rapidly reproduce the DAS-3×3 (within a few minutes) and DAS-5×5 (in about half an hour) reconstructions on a single machine. On a cluster with around 20 CPUs, the reconstruction of DAS-7×7 can be discovered after several hours of computation. Running this approach for an extended period on a cluster not only repeatedly finds DAS-3×3 and DAS-5×5 but also occasionally discovers DAS-7×7 and some previously unreported DAS and non-DAS reconstructions, with and without stacking faults. As summarized in Table 1, all the DAS models (Fig. 2 (a)-(d), DAS-d₈-T¹²,

DAS-d₈-T⁹H^{3-A}, DAS-d₈-T⁹H^{3-B} and DAS-d₈-T⁶H⁶) lost 8 atoms in reconstruction, including 1 inner half-layer atom c and 7 outer half-layer atoms d, respectively. They contain 12 adatoms at the surface in different distributions of T¹², T⁹H^{3-A}, T⁹H^{3-B} and T⁶H⁶, where T/H means the adatom positions and A/B indicates that H position is located at the AA/AB stacking area. Here, the well-known DAS model is cited as DAS-d₈-T¹² to distinguish it from other DAS structures, where d₈ and T¹² indicate that it lost 8 surface atoms in the reconstruction and hold 12 adatoms in the T4 positions. As the non-DAS models shown in Fig 2 (e)-(h), the reconstructed layer and the next inner layer exhibit a complete AB or AA stacking, rather than those with stacking-fault in mixed AA and AB manners. These non-DAS models also undergo the internal dimerization and surface passivation, but lost more surface atoms in number of 10, including 1 inner half-layer atom c and 9 outer half-layer atoms d under the reconstruction. They possess also 12 adatoms in different distributions (AB-d₁₀-T¹², AB-d₁₀-T⁹H³, AA-d₁₀-T¹² and AA-d₁₀-T⁹H³), showing similar pictures to those in the DAS models. In table 1, the dangling bonds (DB), pairs of dimerization (POD) and coverage rate (R_c) for different models of Si(111) surface are listed Table 1 for comparison. The DAS models contain 9 pairs of self-saturated dimers (POD) and 19 total dangling bonds (tot-DB) distributing on the 12 adatoms (ad-DB), 6 unsaturated surface atoms (s-DB) and 1 inner-layer uncovered atom (iL-DB), respectively. However, the non-DAS models contain 12 PODs and 17 tot-DBs distributing on the 12 adatoms, 4 unsaturated surface atoms, and 1 inner-layer uncovered atom.

Table 1. The summarize of the numbers for dangling bonds (ad-DB, s-DB, iL-DB and Tot-DB) and pairs of dimerization (POD) in different models, as well as the coverage rate (R_c) and surface energy (E_s) in unit of meV/Å² for different reconstructions in Si(111) surface.

Systems	ad-DB	s-DB	iL-DB	tot-DB	POD	R _c	E _{surf}	Band gap
Clean-1×1	0	1	0	1	0	0	0	Metal
DAS-3×3	2	0	1	3	3	2/9	-21.5	Metal
DAS-5×5	6	2	1	9	6	12/25	-23.8	Metal
DAS-d ₈ -T ¹²	12	6	1	19	9	12/49	-23.6	Metal
DAS-d ₈ -T ⁹ H ^{3-B}	12	6	1	19	9	12/49	-19.7	0.043 eV
DAS-d ₈ -T ⁹ H ^{3-A}	12	6	1	19	9	12/49	-20.7	0.182 eV
DAS-d ₈ -T ⁶ H ⁶	12	6	1	19	9	12/49	-16.8	Metal
AB-d ₁₀ -T ¹²	12	4	1	17	12	12/49	-16.9	Metal
AB-d ₁₀ -T ⁹ H ³	12	4	1	17	12	12/49	-12.9	0.043 eV
AA-d ₁₀ -T ¹²	12	4	1	17	12	12/49	-13.9	Metal
AA-d ₁₀ -T ⁹ H ³	12	4	1	17	12	12/49	-9.8	0.059 eV

All these models are fully optimized under PBE functional as implemented in the widely used VASP code [59-61] based on a slab model including 3 bulk Si-layers covered by the reconstructed bilayer on the surface and hydrogen on the other side (Atom numbers are 445 and 443 for DAS and non-DAS models). The lattice constants are fixed as those in the optimized bulk silicon as 27.069 Å. The convergence accuracy of energy and force are 10^{-5} eV and 0.01 eV/Å, respectively. The cutoff energy is set to be 400 eV and the k-meshes of $5 \times 5 \times 1/4 \times 4 \times 1/3 \times 3 \times 1$ is used for the $3 \times 3/5 \times 5/7 \times 7$ surface, respectively. The surface energy (E_{surf}) can be evaluated as $E_{surf} = (E_{tot}^{rec-H} - E_{tot}^{1 \times 1-H} \times \frac{S_{tot}^{rec-H}}{S_{tot}^{1 \times 1-H}} - \mu \times N_{surface}) / S_{tot}^{rec-H}$ [62-63], where E_{tot}^{rec-H} and S_{tot}^{rec-H} are the total energy and surface area of the reconstructed system, respectively, while $E_{tot}^{1 \times 1-H}$ and $S_{tot}^{1 \times 1-H}$ are the total energy and surface area of the clean surface in primitive cell (1×1). μ is the average energy calculated from bulk silicon and N accounts only the number of silicon atoms in the surface excluding the reference cell. In present work, the E_{surf} of the clean surface (1×1 -Ad0) is set to be zero as reference. As the results shown in Table 1, all reconstructions are exothermic and more stable than the clean surface. It can be noticed that the ground state for Si(111) surface is the DAS- 5×5 (-23.8 meV/Å²), which has been reported in previous calculations [9]. For the 7×7 reconstructions, the well-known DAS model of DAS-d₈-T¹² (-23.6 meV/Å²) is confirmed to be the most stable one. And the following low-energies ones are DAS-d₈-T⁹H^{3-A}, DAS-d₈-T⁶H^{6-B}, AB-d₁₀-T¹², DAS-d₈-T⁹h^{3-B}, AB-d₁₀-T⁹H³, AA-d₁₀-T¹² and AA-d₁₀-T⁹H³, with energies increase sequentially by just 1-3 meV/Å². It is noticed that the DAS-d₈-T⁶H⁶ and DAS-d₈-T⁹h^{3-B} have been reported in recent literature [17]. They were predicted possessing energies just 3.17 meV/Å² and 7.79 meV/Å² higher than DAS-d₈-T¹², showing same energy order as our present work. The comparison and consistence between our results and those in previous literatures [9, 17] confirmed that our method and settings are reasonable for calculating Si(111) surface.

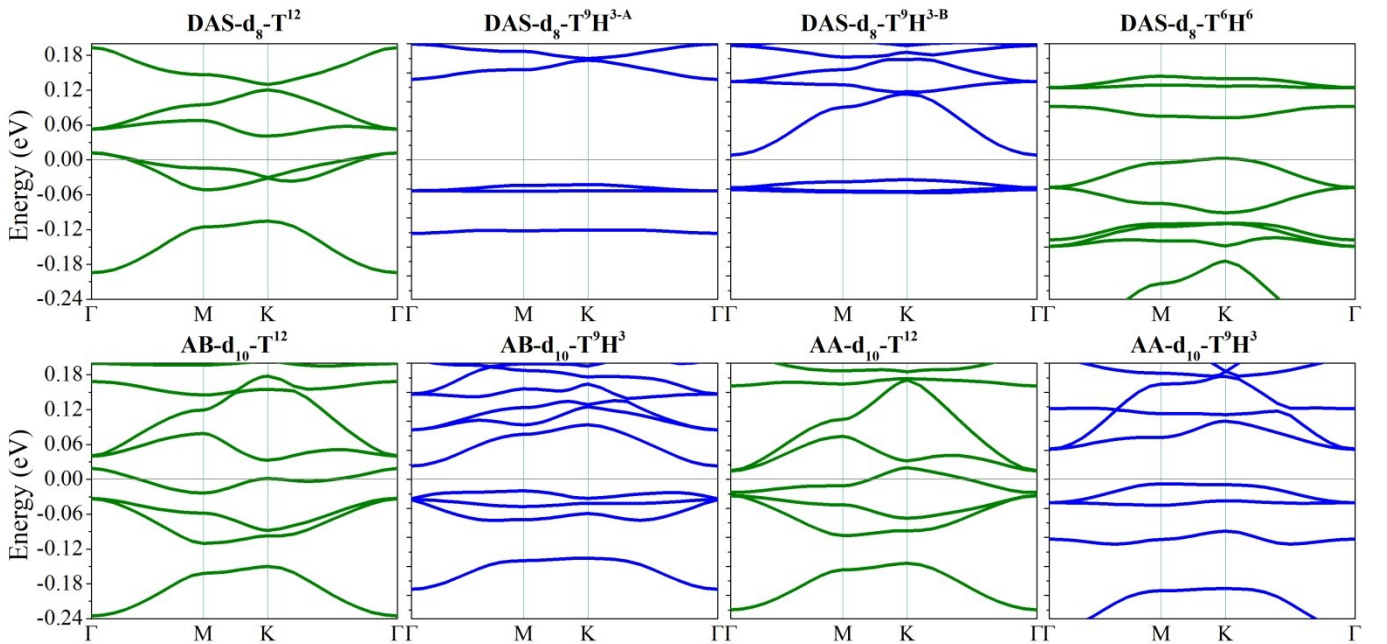


Fig.3. The PBE-based electronic band structures of different reconstructions for Si(111)- 7×7 surface.

As shown in Fig.3, we calculated the electronic band structures of these models based on PBE functional. The results show that DAS-d₈-T¹², DAS-d₈-T⁶H⁶, AB-d₁₀-T¹² and AA-d₁₀-T¹² are metallic phases, with the Fermi-level obviously cross the highest valance band. However, the DAS-d₈-T⁹H^{3-A}, DAS-d₈-T⁹H^{3-B}, AB-d₁₀-T⁹H³ and AA-d₁₀-T⁹H³ are insulators with gaps of 0.043 eV, 0.182 eV, 0.043 eV and 0.059 eV, respectively. At present, the origin of the difference between metals and semiconductors remains unknown, but certain structural patterns can provide insights. In metallic phases, the 12 adatoms are arranged into two equal-sized equilateral triangles (T⁶ and H⁶), whereas in semiconductor phases, they form an equilateral triangle (T⁶) and a reuleaux triangle (T³H³) in different regions. The well-known DAS model DAS-d₈-T¹² has been widely investigated and confirmed to be a metallic phase [7, 33], which is not suitable for explaining the experimentally observed metal-insulating transition [7, 37-46] in the surface of Si(111)-7×7. Here, our work also concludes that the well-known DAS model DAS-d₈-T¹² is metallic, further demonstrating the reliability of our method. Notably, we have identified four semiconductor phases, for the first time in theoretical views, which may provide insights into the metal-to-insulator phase transition in the reconstructed Si(111)-7×7 surface.

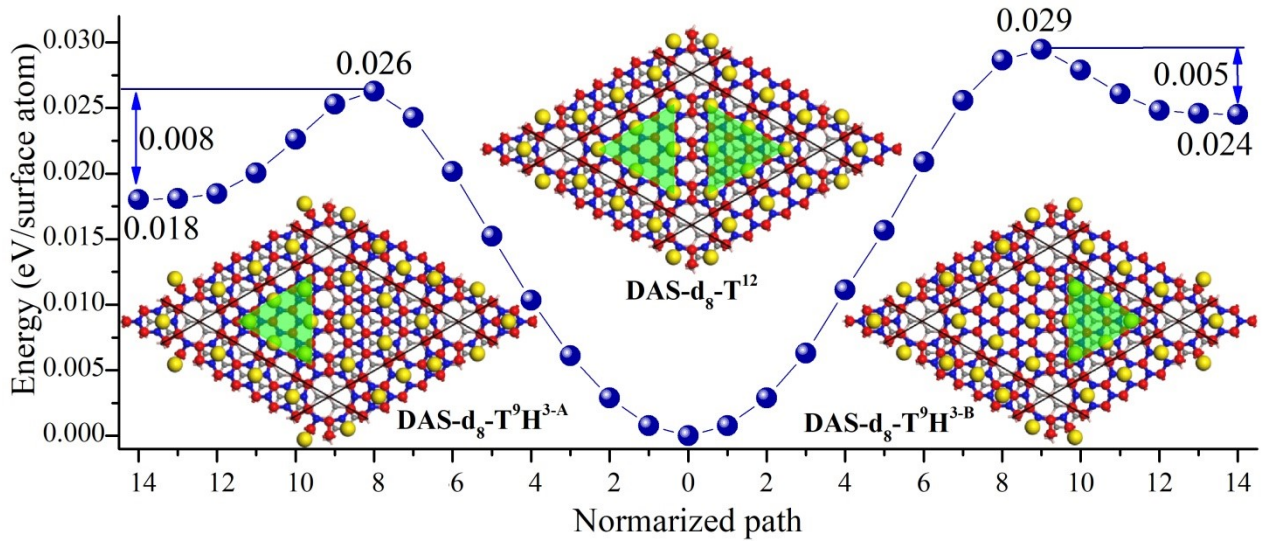


Fig.4 The energies and barriers on the transition pathways from the metallic DAS-d₈-T¹² to the insulating DAS-d₈-T⁹H^{3-A} (left) and DAS-d₈-T⁹H^{3-B} (right).

In the previous discussion, we mentioned that these reconstruction models can be classified into two groups: DAS and non-DAS. The only difference between structures within the same group lies in the distribution of the 12 adatoms. Notably, different distributions of these 12 atoms can be interconverted through surface diffusion. As shown in Fig. 4, we aim to discuss the possibility of structural phase transitions from the perspective of the potential energy surface and, based on this, provide an explanation for the transition of the Si(111) 7×7 reconstruction from a metallic phase to an insulating phase. It is clearly that the energy barriers from the metallic DAS-d₈-T¹² to the semiconducting DAS-d₈-T⁹H^{3-A} and DAS-d₈-T⁹H^{3-B} are 26 meV and 29 meV per surface atom (102). This energy magnitude indicates that the

classic DAS model, the metallic DAS-d₈-T¹², of the Si(111) surface has the potential to transition into two semiconductor phases under high-temperature conditions. Moreover, these two new phases are protected by energy barriers of 8 meV and 5 meV per surface atom, respectively, preventing spontaneous transition back to the metallic ground-state structure of DAS-d₈-T¹².

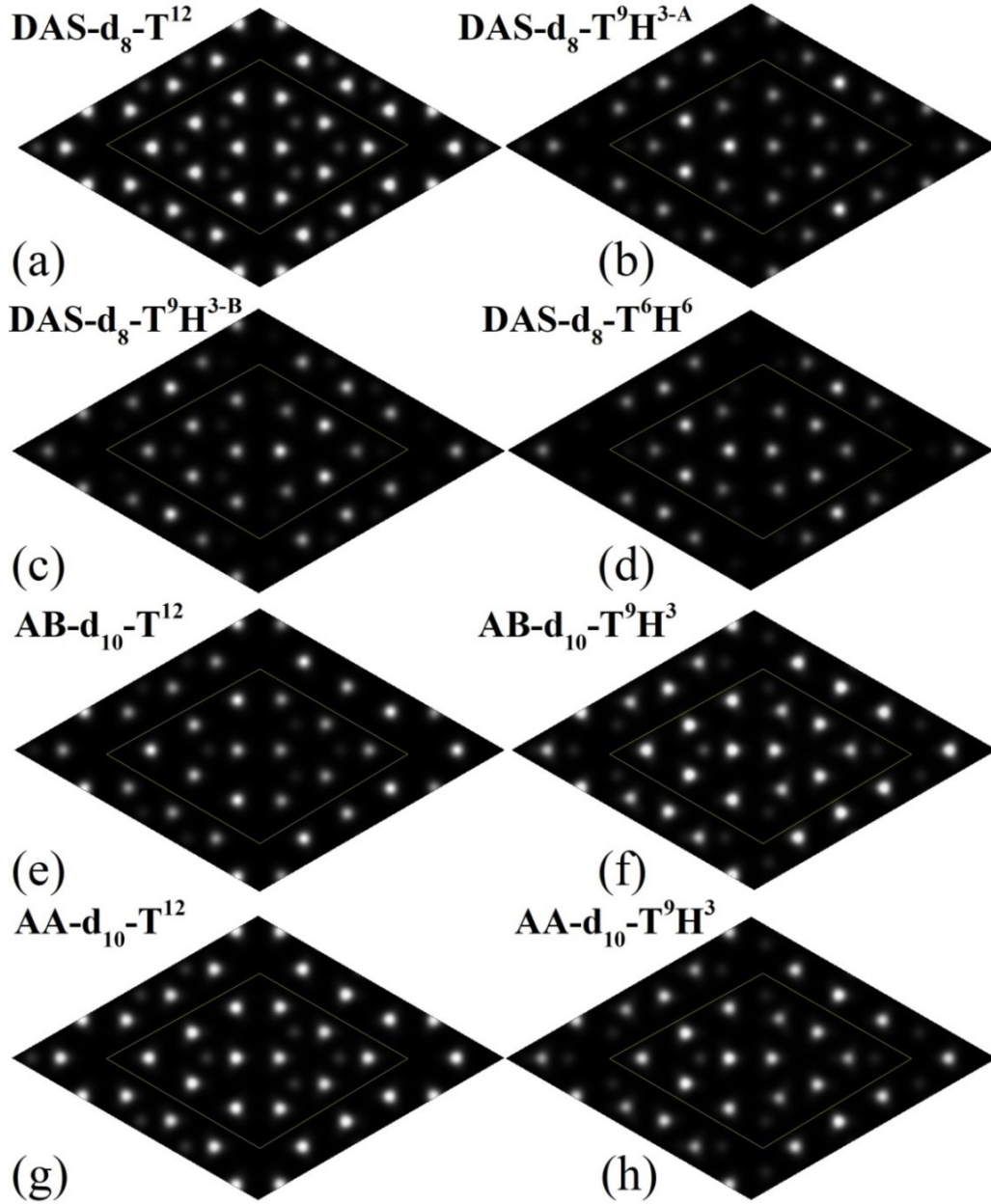


Fig.5 The simulated STM images for different reconstructions for Si(111)-7×7 surface with and without stacking fault.

Finally, we simulated the STM patterns of these surface reconstructions to provide a reference for their experimental identification. As shown in Fig 5, their STM patterns are difficult to distinguish without careful observation. In other words, at low experimental resolution, these structures may be misidentified in STM images. This might explain why the semiconductor phase observed in experiments is still commonly interpreted using structure the well-known DAS model of DAS-d₈-T¹². Upon careful comparison, we can distinguish DAS-d₈-T¹² and DAS-d₈-T⁶H⁶ among the DAS models based on their primary bright spots, which distribute as two equilateral triangles and two Reuleaux triangles, respectively. In contrast, the

primary bright spots in $\text{DAS-d}_8\text{-T}^9\text{H}^{3\text{-A}}$ and $\text{DAS-d}_8\text{-T}^9\text{H}^{3\text{-B}}$ each contain both an equilateral triangle and a Reuleaux triangle. For the non-DAS models ($\text{AB-d}_{10}\text{-T}^{12}$, $\text{AB-d}_{10}\text{-T}^9\text{H}^3$, $\text{AA-d}_{10}\text{-T}^{12}$ and $\text{AA-d}_{10}\text{-T}^9\text{H}^3$), it is easy to distinguish the distribution of the 12 adatoms, but distinguishing between stacking manners $\text{AB-d}_{10}\text{-T}^{12}$ and $\text{AA-d}_{10}\text{-T}^{12}$, as well as $\text{AB-d}_{10}\text{-T}^9\text{H}^3$ and $\text{AA-d}_{10}\text{-T}^9\text{H}^3$, remains challenging. Notably, relying solely on the primary bright spots makes it difficult to distinguish $\text{DAS-d}_8\text{-T}^{12}$ from $\text{AB-d}_{10}\text{-T}^{12}$ and $\text{AA-d}_{10}\text{-T}^{12}$, as all three contain paired equilateral triangles. However, $\text{AB-d}_{10}\text{-T}^{12}$ and $\text{AA-d}_{10}\text{-T}^{12}$ exhibit secondary bright spots in only one region with a triangular distribution, whereas $\text{DAS-d}_8\text{-T}^{12}$ features six double-triangle secondary bright spots distributed across two regions.

In summary, it has demonstrated that the 7×7 reconstructions of the Si(111) surface can be effectively predicted using graph theory as implemented in the RG^2 code. Our approach successfully identifies both metallic and insulating reconstructions, including configurations with and without stacking faults, all exhibiting comparable energetic stability to the well-known DAS model. Based on first-principles calculations, the $\text{DAS-d}_8\text{-T}^{12}$, $\text{DAS-d}_8\text{-T}^6\text{H}^6$, $\text{AB-d}_{10}\text{-T}^{12}$, and $\text{AA-d}_{10}\text{-T}^{12}$ are confirmed as metallic phases, while $\text{DAS-d}_8\text{-T}^9\text{H}^{3\text{-A}}$, $\text{DAS-d}_8\text{-T}^9\text{H}^{3\text{-B}}$, $\text{AB-d}_{10}\text{-T}^9\text{H}^3$ and $\text{AA-d}_{10}\text{-T}^9\text{H}^3$ are semiconductors with gaps of 0.043 eV, 0.182 eV, 0.043 eV and 0.059 eV, respectively. These predicted structures not only reproduce the characteristic STM patterns observed in experiments but also provide a plausible explanation for the long-standing discrepancy between theoretical predictions and the experimentally observed insulating features. Our results highlight the predictive power of graph theory in complex surface reconstructions and suggest that alternative low-energy insulating phases may coexist with the metallic DAS model on the Si(111)- 7×7 surface.

Acknowledgments

Chaoyu He acknowledges Prof. Chris J. Pickard for discussion about the calculation of surface energy, as well as Prof. J. E. Demuth for discussions on the DAS models and the issues within it. This work is supported by the National Natural Science Foundation of China (Grant Nos. 52372260, and 12204397, 12374046), the Youth Science and Technology Talent Project of Hunan Province (Grant No. 2022RC1197) and the Research Foundation of Education Bureau of Hunan Province, China (Grant No. 24A0121), the Science Fund for Distinguished Young Scholars of Hunan Province of China (No.2024JJ2048).

Reference

- [1] R. S. Becker, J. A. Golovchenko, and B. S. Swartzentruber, Tunneling Images of Germanium Surface Reconstructions and Phase Boundaries, *Physical Review Letters* 54, 2678 (1985).
- [2] V. Cherepanov and B. Voigtländer, Influence of material, surface reconstruction, and strain on diffusion at the Ge(111) surface, *Physical Review B* 69, 125331 (2004).
- [3] J. Schardt, J. Bernhardt, U. Starke, and K. Heinz, Crystallography of the (3×3) surface reconstruction of

- 3C-SiC(111), 4H-SiC(0001), and 6H-SiC(0001) surfaces retrieved by low-energy electron diffraction, *Physical Review B* 62, 10335 (2000).
- [4] R. S. Becker, J. A. Golovchenko, D. R. Hamann, and B. S. Swartzentruber, Real-Space Observation of Surface States on Si(111) 7×7 with the Tunneling Microscope, *Physical Review Letters* 55, 2032 (1985).
- [5] R. J. Hamers, R. M. Tromp, and J. E. Demuth, Surface Electronic Structure of Si(111)- (7×7) Resolved in Real Space, *Physical Review Letters* 56, 1972 (1986).
- [6] R. E. Schlier and H. E. Farnsworth, Structure and Adsorption Characteristics of Clean Surfaces of Germanium and Silicon, *The Journal of Chemical Physics* 30, 917 (1959).
- [7] S. Modesti, P. M. Sheverdyeva, P. Moras, C. Carbone, M. Caputo, M. Marsi, E. Tosatti, and G. Profeta, Low-temperature insulating phase of the Si(111)- 7×7 surface, *Physical Review B* 102, 035429 (2020).
- [8] T. Eguchi and Y. Hasegawa, High Resolution Atomic Force Microscopic Imaging of the Si(111)- (7×7) Surface: Contribution of Short-Range Force to the Images, *Physical Review Letters* 89, 266105 (2002).
- [9] R. A. Zhachuk and J. Coutinho, Crucial role of vibrational entropy in the Si(111)- 7×7 surface structure stability, *Physical Review B* 105, 245306 (2022).
- [10] I. Štich, M. C. Payne, R. D. King-Smith, J. S. Lin, and L. J. Clarke, Ab initio total-energy calculations for extremely large systems: Application to the Takayanagi reconstruction of Si(111), *Physical Review Letters* 68, 1351 (1992).
- [11] K. D. Brommer, M. Needels, B. Larson, and J. D. Joannopoulos, Ab initio theory of the Si(111)- (7×7) surface reconstruction: A challenge for massively parallel computation, *Physical Review Letters* 68, 1355 (1992).
- [12] S.-W. Wang, C.-R. Hsing, and C.-M. Wei, Expedite random structure searching using objects from Wyckoff positions, *The Journal of Chemical Physics* 148 (2018).
- [13] M. K. Bisbo and B. Hammer, Efficient Global Structure Optimization with a Machine-Learned Surrogate Model, *Physical Review Letters* 124, 086102 (2020).
- [14] M. N. Bauer, M. I. J. Probert, and C. Panosetti, Systematic Comparison of Genetic Algorithm and Basin Hopping Approaches to the Global Optimization of Si(111) Surface Reconstructions, *The Journal of Physical Chemistry A* 126, 3043 (2022).
- [15] X. Du, J. K. Damewood, J. R. Lunger, R. Millan, B. Yildiz, L. Li, and R. Gómez-Bombarelli, Machine-learning-accelerated simulations to enable automatic surface reconstruction, *Nature Computational Science* 3, 1034 (2023).
- [16] F. Brix, M.-P. Verner Christiansen, and B. Hammer, Cascading symmetry constraint during machine learning-enabled structural search for sulfur-induced Cu(111)- (43×43) surface reconstruction, *The Journal of Chemical Physics* 160 (2024).

- [17] Y. Han, C. Ding, J. Wang, H. Gao, J. Shi, S. Yu, Q. Jia, S. Pan, and J. Sun, Efficient crystal structure prediction based on the symmetry principle, *Nature Computational Science* (2025).
- [18] J. D. Levine, S. H. McFarlane, and P. Mark, Si (111) (7×7) surface structure: Calculations of LEED intensity and comparison with experiment, *Physical Review B* 16, 5415 (1977).
- [19] M. J. Cardillo, Nature of the Si(111) 7×7 reconstruction, *Physical Review B* 23, 4279 (1981).
- [20] G. Binnig, H. Rohrer, C. Gerber, and E. Weibel, 7×7 Reconstruction on Si(111) Resolved in Real Space, *Physical Review Letters* 50, 120 (1983).
- [21] P. A. Bennett, L. C. Feldman, Y. Kuk, E. G. McRae, and J. E. Rowe, Stacking-fault model for the Si(111)-(7×7) surface, *Physical Review B* 28, 3656 (1983).
- [22] E. G. McRae, Surface stacking sequence and (7×7) reconstruction at Si(111) surfaces, *Physical Review B* 28, 2305 (1983).
- [23] K. Takayanagi, Y. Tanishiro, M. Takahashi, and S. Takahashi, Structural analysis of Si(111) - 7×7 by UHV - transmission electron diffraction and microscopy, *Journal of Vacuum Science & Technology A* 3, 1502 (1985).
- [24] R. Zhachuk, B. Olshanetsky, J. Coutinho, and S. Pereira, Electronic effects in the formation of apparently noisy scanning tunneling microscopy images of Sr on Si(111)- 7×7 , *Physical Review B* 81, 165424 (2010).
- [25] G.-X. Qian and D. J. Chadi, Si(111)- 7×7 surface: Energy-minimization calculation for the dimer-atom-stacking-fault model, *Physical Review B* 35, 1288 (1987).
- [26] H. Lim, K. Cho, I. Park, J. D. Joannopoulos, and E. Kaxiras, Ab initio study of hydrogen adsorption on the Si(111)-(7×7) surface, *Physical Review B* 52, 17231 (1995).
- [27] D. R. Alfonso, C. Noguez, D. A. Drabold, and S. E. Ulloa, First-principles studies of hydrogenated Si(111)- 7×7 , *Physical Review B* 54, 8028 (1996).
- [28] J. Ortega, F. Flores, and A. L. Yeyati, Electron correlation effects in the Si(111)- 7×7 surface, *Physical Review B* 58, 4584 (1998).
- [29] F. J. Giessibl, S. Hembacher, H. Bielefeldt, and J. Mannhart, Subatomic Features on the Silicon (111)-(7×7) Surface Observed by Atomic Force Microscopy, 289, 422 (2000).
- [30] R. Schillinger, C. Bromberger, H. J. Jansch, H. Kleine, O. Köhlert, C. Weindel, and D. Fick, Metallic Si(111)-(7×7)-reconstruction: A surface close to a Mott-Hubbard metal-insulator transition, *Physical Review B* 72, 115314 (2005).
- [31] J. A. McGuire, M. B. Raschke, and Y. R. Shen, Electron Dynamics of Silicon Surface States: Second-Harmonic Hole Burning on Si(111)-(7×7) *Physical Review Letters* 96, 087401 (2006).
- [32] Y. Cho and R. Hirose, Atomic Dipole Moment Distribution of Si Atoms on a Si(111)-(7×7) Surface

- Studied Using Noncontact Scanning Nonlinear Dielectric Microscopy, *Physical Review Letters* 99, 186101 (2007).
- [33] X.-Y. Ren, C.-Y. Niu, S. Yi, S. Li, and J.-H. Cho, Hydrogen adsorption induced nanomagnetism at the Si(111)-(7×7) surface, *Physical Review B* 98, 195424 (2018).
- [34] A. P. Bartók, J. Kermode, N. Bernstein, and G. Csányi, Machine Learning a General-Purpose Interatomic Potential for Silicon, *Physical Review X* 8, 041048 (2018).
- [35] Y. Shen, S. I. Morozov, K. Luo, Q. An, and W. A. Goddard III, Deciphering the Atomistic Mechanism of Si(111)-7×7 Surface Reconstruction Using a Machine-Learning Force Field, *Journal of the American Chemical Society* 145, 20511 (2023).
- [36] L. Hu, B. Huang, and F. Liu, Atomistic Mechanism Underlying the Si(111)-(7×7) Surface Reconstruction Revealed by Artificial Neural-Network Potential, *Physical Review Letters* 126, 176101 (2021).
- [37] R. I. G. Uhrberg, T. Kaurila, and Y. C. Chao, Low-temperature photoemission study of the surface electronic structure of Si(111)7×7, *Physical Review B* 58, R1730 (1998).
- [38] P. Martensson, W.-X. Ni, G. V. Hansson, J. M. Nicholls, and B. Reihl, Surface electronic structure of Si(111)7×7-Ge and Si(111)5×5-Ge studied with photoemission and inverse photoemission, *Physical Review B* 36, 5974 (1987).
- [39] J. Mysliveček, A. Stróżecka, J. Steffl, P. Sobotík, I. Ošt’ádal, and B. Voigtländer, Structure of the adatom electron band of the Si(111)-7×7 surface, *Physical Review B* 73, 161302 (2006).
- [40] J. E. Demuth, B. N. J. Persson, and A. J. Schell-Sorokin, Temperature-Dependent Surface States and Transitions of Si(111)-7×7, *Physical Review Letters* 51, 2214 (1983).
- [41] R. Losio, K. N. Altmann, and F. J. Himpsel, Fermi surface of Si(111)7×7, *Physical Review B* 61, 10845 (2000).
- [42] I. Barke, F. Zheng, A. R. Konicek, R. C. Hatch, and F. J. Himpsel, Electron-Phonon Interaction at the Si(111)-7×7 Surface, *Physical Review Letters* 96, 216801 (2006).
- [43] M. E. Dávila, J. Ávila, I. R. Colambo, D. B. Putungan, D. P. Woodruff, and M. C. Asensio, New insight on the role of localisation in the electronic structure of the Si(111)(7×7) surfaces, *Scientific Reports* 11, 15034 (2021).
- [44] S. Modesti, H. Gutzmann, J. Wiebe, and R. Wiesendanger, Correction of systematic errors in scanning tunneling spectra on semiconductor surfaces: The energy gap of Si(111)-7×7 at 0.3 K, *Physical Review B* 80, 125326 (2009).
- [45] A. B. Odobescu and S. V. Zaitsev-Zotov, Energy gap revealed by low-temperature scanning-tunnelling spectroscopy of the Si(111)-7×7 surface in illuminated slightly doped crystals, *Journal of Physics:*

Condensed Matter 24, 395003 (2012).

[46] A. B. Odobescu, A. A. Maizlakh, and S. V. Zaitsev-Zotov, Electron correlation effects in transport and tunneling spectroscopy of the Si(111)-7×7 surface, *Physical Review B* 92, 165313 (2015).

[47] A. L. Efros and B. I. Shklovskii, Coulomb gap and low temperature conductivity of disordered systems, *Journal of Physics C: Solid State Physics* 8, L49 (1975).

[48] J. Heyd, G. E. Scuseria, and M. Ernzerhof, Hybrid functionals based on a screened Coulomb potential, *The Journal of Chemical Physics* 118, 8207 (2003).

[49] L. Hedin, New Method for Calculating the One-Particle Green's Function with Application to the Electron-Gas Problem, *Physical Review* 139, A796 (1965).

[50] J. E. Demuth, Experimental Evidence for a New Two-Dimensional Honeycomb Phase of Silicon: A Missing Link in the Chemistry and Physics of Silicon Surfaces?, *The Journal of Physical Chemistry C* 124, 22435 (2020).

[51] J. E. Demuth, Evidence for Symmetry Breaking in the Ground State of the Si(111)-7×7: The Origin of Its Metal–Insulator Transition, *physica status solidi (b)* 257, 2000229 (2020).

[52] J. E. Demuth, A re-evaluation of diffraction from Si(111) 7 × 7: decoding the encoded phase information in the 7 × 7 diffraction pattern, *Physical Chemistry Chemical Physics* 23, 8043 (2021).

[53] R. A. Zhachuk and J. Coutinho, Comment on “Experimental Evidence for a New Two-Dimensional Honeycomb Phase of Silicon: A Missing Link in the Chemistry and Physics of Silicon Surfaces?”, *The Journal of Physical Chemistry C* 126, 866 (2022).

[54] X. Shi, C. He, C. J. Pickard, C. Tang, and J. Zhong, Stochastic generation of complex crystal structures combining group and graph theory with application to carbon, *Physical Review B* 97, 014104 (2018).

[55] C. He, X. Shi, S. J. Clark, J. Li, C. J. Pickard, T. Ouyang, C. Zhang, C. Tang, and J. Zhong, Complex Low Energy Tetrahedral Polymorphs of Group IV Elements from First Principles, *Physical Review Letters* 121, 175701 (2018).

[56] S. Li, X. Shi, J. Li, C. He, T. Ouyang, C. Tang, and J. Zhong, Spin-orbital coupling induced isolated flat band in bismuthene with k-dependent spin texture, *Physical Review B* 110, 115115 (2024).

[57] C. He, S. Li, Y. Zhang, Z. Fu, J. Li, and J. Zhong, Isolated zero-energy flat bands and intrinsic magnetism in carbon monolayers, *Physical Review B* 111, L081404 (2025).

[58] C. He, Y. Liao, T. Ouyang, H. Zhang, H. Xiang, and J. Zhong, Flat-band based high-temperature ferromagnetic semiconducting state in the graphitic C₄N₃ monolayer, *Fundamental Research* 5, 138 (2025).

[59] G. Kresse and J. Furthmüller, Efficient iterative schemes for ab initio total-energy calculations using a plane-wave basis set, *Physical Review B* 54, 11169 (1996).

[60] J. P. Perdew, K. Burke, and M. Ernzerhof, Generalized Gradient Approximation Made Simple, *Physical*

Review Letters 77, 3865 (1996).

[61]G. Kresse and D. Joubert, From ultrasoft pseudopotentials to the projector augmented-wave method, *Physical Review B* 59, 1758 (1999).

[62]R. Zhachuk, S. Teys, and J. Coutinho, Strain-induced structure transformations on Si(111) and Ge(111) surfaces: A combined density-functional and scanning tunneling microscopy study, *The Journal of Chemical Physics* 138 (2013).

[63]R. Zhachuk, J. Coutinho, A. Dolbak, V. Cherepanov, and B. Voigtländer, Si(111) strained layers on Ge(111): Evidence for $c(2\times 4)$ domains, *Physical Review B* 96, 085401 (2017).

[64]M. Smeu, H. Guo, W. Ji, and R. A. Wolkow, Electronic properties of Si(111)- 7×7 and related reconstructions: Density functional theory calculations, *Physical Review B* 85, 195315 (2012).